

Lamin B1 regulates RNA splicing factor expression by modulating the spatial positioning and chromatin interactions of the *ETS1* gene locus

Geun-Seup Shin*, Ah-Ra Jo*, Jinho Kim, Ji-Young Kim, Chul-Hong Kim, Mi-Jin An, Hyun-Min Lee, Yuna Park, Yujeong Hwangbo and Jung-Woong Kim

Department of Life Science, Chung-Ang University, Seoul, Republic of Korea

ABSTRACT

Lamin B1, a crucial component of the nuclear lamina, plays a pivotal role in chromatin organization and transcriptional regulation in eukaryotic cells. While recent studies have highlighted the connection between Lamin B1 and RNA splicing regulation, the precise molecular mechanisms remain elusive. In this study, we demonstrate that Lamin B1 depletion leads to a global reduction in splicing factor expression, as evidenced by analysis of multiple RNA-seq datasets. Motif analysis suggests that members of the ETS transcription factor family likely bind to the promoter regions of these splicing factors. Further analysis using transcription factor databases and ChIP-seq data identified *ETS1* as a key regulator of splicing factor expression. Hi-C sequencing revealed that the loss of Lamin B1 disrupts inter-LAD chromatin interactions near the *ETS1* gene locus, resulting in its downregulation. These findings suggest that Lamin B1 indirectly regulates RNA splicing by sustaining proper *ETS1* expression, uncovering a novel link between nuclear architecture, gene regulation, and RNA splicing.

ARTICLE HISTORY

Received 8 October 2024
Revised 22 January 2025
Accepted 30 January 2025

KEYWORDS

Lamin B1; *ETS1*; RNA splicing; chromatin organization; upstream regulator

Introduction

In eukaryotic cells, Lamin proteins form a mesh-like structure known as the nuclear lamina beneath the inner nuclear membrane, essential for maintaining nuclear integrity (Dechat et al. 2008; Kim et al. 2024). Among these, B-type Lamins, particularly Lamin B1, play a central role in tethering specific regions of chromatin, called lamina-associated domains (LADs), to the nuclear periphery (Goldman et al. 2002; Yang et al. 2011). Lamin B1 establishes a transcriptionally repressive environment, as genes located within these regions are typically inactive (Chang et al. 2022). Moreover, the expression level of Lamin B1 affects chromatin compaction, which in turn modulates its accessibility to transcriptional machinery (Kaneshiro et al. 2023). For instance, depletion of Lamin B1 has been shown to enhance chromatin mobility and decompaction, leading to abnormal gene regulation by altering interactions between chromatin and regulatory proteins (Pujadas Liwag et al. 2024). These dysregulated genes can impact various biological processes, either directly or indirectly.


Previous studies have demonstrated that the loss of Lamin B1 induces aberrant alternative splicing in numerous genes, likely due to changes in chromatin compaction

and spatial organization (Tang et al. 2008; Schor et al. 2012; Camps et al. 2014). Conversely, overexpression of Lamin B1 also disrupts standard RNA splicing patterns in several genes, potentially contributing to the development of autosomal dominant leukodystrophy (ADLD) (Bartoletti-Stella et al. 2015). One study found that the sequestration of splicing factors near the nuclear lamina can impair their splicing activity, highlighting the importance of spatial proximity between Lamin B1 and splicing factors in the regulation of RNA splicing (Vester et al. 2022). These findings suggest a strong link between Lamin B1 and RNA splicing regulation, though the exact molecular mechanisms remain unclear.

Alternative splicing is a key mechanism in gene expression that enables a single gene to generate multiple protein isoforms by selectively including or excluding exons, thus increasing protein diversity without additional genes (Liu et al. 2022). Since this process is governed by various splicing factors, dysregulation of these factors can lead to altered splicing patterns, potentially contributing to disease (Zhang and Manley 2013; Li et al. 2021; Lee et al. 2024). Splicing factors often exhibit coordinated expression patterns, and this synchronized

CONTACT Jung-Woong Kim  jungkim@cau.ac.kr  Department of Life Science, Chung-Ang University, Seoul, Republic of Korea

*These authors contributed equally.

 Supplemental data for this article can be accessed online at <https://doi.org/10.1080/19768354.2025.2465325>.

© 2025 The Author(s). Published by Informa UK Limited, trading as Taylor & Francis Group

This is an Open Access article distributed under the terms of the Creative Commons Attribution-NonCommercial License (<http://creativecommons.org/licenses/by-nc/4.0/>), which permits unrestricted non-commercial use, distribution, and reproduction in any medium, provided the original work is properly cited. The terms on which this article has been published allow the posting of the Accepted Manuscript in a repository by the author(s) or with their consent.

regulation is essential for maintaining proper RNA splicing during dynamic cellular processes (Dominguez et al. 2016; Mehlferber et al. 2023; Podszylow-Bartnicka and Neugebauer 2023). For instance, it has been shown that splicing factor genes display periodic expression during cell cycle progression, a pattern closely linked to periodic splicing events (Dominguez et al. 2016). Moreover, the simultaneous upregulation or downregulation of splicing factors is frequently observed during cancer progression (Koedoot et al. 2019), indicating that their expression may be co-regulated as part of broader transcriptional programs.

The ETS family of transcription factors plays a critical role in various biological processes, including cell differentiation, proliferation, growth, and apoptosis (Oikawa and Yamada 2003; Yang et al. 2024). Most members of the ETS family function as transcriptional activators, binding to GGAA/T motifs in the promoters of target genes such as p53, Bcl2, and JunB (Wasylyk et al. 1993; Sementchenko and Watson 2000; Sharrocks 2001). The ETS family comprises 28 members, including ELF1, ERG, ETV6, ELK3, ELK4, FLI1, and ETS1, each with distinct roles under different conditions (Maroulakou and Bowe 2000; Yang et al. 2024). Recent research has shown that ERG and FLI1 influence RNA splicing through cooperative interaction with the splicing regulator RBFOX2 (Saulnier et al. 2021). Furthermore, ETV6 has been found to regulate the expression of splicing factors via the ERK and AKT pathways (Latorre et al. 2019), highlighting the potential impact of ETS family members on RNA splicing.

In this study, we discovered that the loss of Lamin B1 led to a global misregulation of genes involved in RNA splicing across various cell types. To identify potential upstream regulators of splicing factors, we performed a *de novo* motif analysis using promoter sequences of splicing factor genes, identifying the ETS transcription factor family as a candidate. Among the ETS family members, Lamin B1 depletion resulted in the downregulation of ELF1, ETS1, ELK3, and ELK4. Further analysis confirmed that only ETS1 directly regulates splicing factor genes. Hi-C sequencing revealed that Lamin B1 depletion disrupted inter-LAD chromatin interactions surrounding the ETS1 gene locus, leading to reduced ETS1 expression. Our findings suggest that the loss of Lamin B1 alters inter-LAD interactions, which in turn impacts ETS1 expression, thereby regulating splicing factor genes at an upstream level.

Materials and methods

Cell cultures

All cell culture reagents used in this study were obtained from Welgene (Seoul, Republic of Korea). MRC5 cells,

human normal lung cells, were purchased from the Korean Cell Line Bank (Seoul, Republic of Korea). MRC5 cells were maintained in DMEM supplemented with 10% fetal bovine serum (FBS), 1% penicillin/streptomycin at 37 °C in an incubator with 5% CO₂ at a humidified atmosphere.

Generation of knockout (KO) stable cell lines

The sgRNA sequence targeting *LMNB1* was designed using the sgRNA prediction tool (<http://crispr.mit.edu>). 20 bp guide sequences are indicated in Supplemental Figure 1. Each oligonucleotide was phosphorylated and annealed using T4 polynucleotide kinase (NEB, MA, USA). The annealed oligos were then ligated into a BsmBI-digested lentiCRISPRv2 vector purchased from Addgene. Cells transfected with the CRISPR vector were selected with 1 µg/ml of puromycin for 4–7 days, followed by a recovery period of approximately 5 days. The sequence of the single clone was confirmed through DNA sequencing.

Total RNA isolation

Total RNA was extracted using the TRIzol solution (15596018, Invitrogen, CA, USA) following the manufacturer's instructions. The contaminated genomic DNA was cleared by mixing 20 units of RNase-free DNase I (New England Biolabs) and 4 units of RNase inhibitor (New England Biolabs) with DEPC-treated water from 10 µg of total RNA. The reaction mixture was incubated at 37°C for 1 hour followed by 10 minutes at 50°C. All RNA extracts showed an OD260:OD280 ratio between 1.8 and 2.0, confirming clear RNA extraction. The purity was assessed by Agilent 2100 Bioanalyzer using the RNA 6000 Nano Chip (Agilent Technologies, Santa Clara, CA). And RNA quantitation was performed using Thermo scientific Multiskan GO microplate reader with µDrop™ Plate (Waltham, MA).

RNA sequencing and bioinformatical analysis

According to the manufacturer's instructions, the TruSeq mRNA Library Prep Kit (Illumina, Inc., USA) generated the RNA-seq library. To be brief, 100 ng of total cells were extracted, and then reverse transcription was carried out using an oligo-dT primer that had an Illumina-compatible sequence at its 5' end. After degradation of the RNA template, a random primer with an Illumina-compatible linker sequence at its 5' end started the second strand synthesis. The AMPure magnetic beads (A63881, Beckman Coulter, CA, USA) were used to remove all reaction components from the double-stranded library during purification. The library was amplified to

include all of the adapter sequences required for cluster generation. The finished library is purified from PCR components. High-throughput sequencing was carried out as paired-end 101 sequencing reads using NextSeq 500 (Illumina, Inc., USA).

In addition to our MRC5 RNA-seq data, we also analyzed the following publicly available RNA-seq datasets: *LMNB1* knockout (*LMNB1*^{-/-}) MDA-MB-231 (GSE124409) (Chang et al. 2022), *Lmnb1* KD MLE12 (GSE94680) (Jia et al. 2019), *ETS1* KD DU145 (GSE59020) (Plotnik et al. 2014), *ETS1* KD SCC25 (GSE109886) (Gluck et al. 2019). All datasets are compared with the control or wild-type (WT) group.

STAR (v.2.7.1a) was used to align mRNA-Seq reads. Indices were generated from either the genome assembly sequence or representative transcript sequences for alignment to the genome and transcriptome. The alignment file was used to assemble transcripts, estimate their abundances, and detect gene expression differences using RSEM (v.1.3.3). Differentially expressed transcripts were identified using EdgeR (v.3.36.0) within R version 4.1.0 (R development Core Team, 2011) using the R package.

cDNA synthesis and reverse transcription quantitative PCR (RT-qPCR)

Oligo-dT (6110A, Takara) was used as the primer for the initial step of cDNA synthesis. 500 ng RNA was mixed with 1 μ l of oligo dT, and distilled water, then preheated at 65°C for 5 minutes to denature the RNA secondary structures. Before adding 10 mM DTT, 4 μ l of 5X PrimeScript buffer, and 200 units of PrimeScript reverse transcriptase (#RR036A, PrimeScript™ RT Master Mix, Takara) to make a total volume of 20 μ l, the mixture was quickly cooled down to 4°C. The reverse transcription was carried out by incubating the mixture at 25°C for 5 minutes, followed by 60 minutes at 42°C, and the reaction was terminated by heating at 70°C for 15 minutes. And then, the stock of cDNA was kept at -20°C. Following the manufacturer's instructions, real-time quantitative PCR was performed using the CFX96 Real-Time PCR Detection System (Bio-Rad) and iQ SYBR Green PCR Supermix (#1708880, Bio-Rad). Melting curve analysis confirmed the specificity of the amplified products. The β -actin gene was used as a reference for normalization, and relative mRNA expression levels were calculated using the 2^{-($\Delta\Delta C_t$)} method. The primer sequences are presented in Supplementary Table 1.

Bioinformatical analysis of ATAC, ChIP, and Hi-C sequencing

We utilized and reanalyzed the publicly available ATAC-seq results in WT and *LMNB1*^{-/-} MDA-MB-231 cells

(GSE124409) (Chang et al. 2022). Moreover, we analyzed the following publicly available ChIP-seq datasets: Lamin A ChIP-seq in WT and *LMNB1*^{-/-} MDA-MB-231 (GSE124409) (Chang et al. 2022), ETS1, ELF1, and ELK4 ChIP-seq in WT DU145 (GSE59021) (Plotnik et al. 2014), ETS1 ChIP-seq in WT PANC1 (GSE59021) (Plotnik et al. 2014). To generate Lamin A ChIP-seq data, the read counts were normalized based on the input read number.

For the processing of ATAC-seq data and Lamin A/C and ETS1 ChIP-seq data, all reads in FASTQ format were aligned to the GRCh38.p13.103 human genome using Bowtie2 (ver 2.4.4) and redundant reads removed. After confirming the consistency between each replicate, we generated the bigwig track for visualization with IGV (ver.2.15.2).

For TAD analysis, insulation scores were calculated for each 40 Kb bin, and TAD boundaries were determined at the valleys of the insulation profiles. Boundaries with an FDR exceeding 1×10^{-6} and TADs smaller than 200 Kb were excluded for further analysis.

Immunoblot

The cells were lysed in a solution including 0.1% sodium dodecyl sulfate (SDS), 1% Nonidet P-40, 1 mM PMSF, 1X PIC, 1% Triton X-100, 150 mM NaCl and 50 mM Tris-HCl (pH 7.5). After homogenizing on ice, the cell suspensions were centrifuged at 15,000 g for 10 minutes at 4°C. The protein samples were electrophoresed on a 10% SDS-PAGE and transferred to a nitrocellulose membrane (Amersham; Cytiva, US). The membrane was blocked using 5% skim milk in TBST buffer (137 mM NaCl, 20 mM Tris-HCl, pH 7.6, and 0.1% Tween-20) and incubated overnight at 4°C with a diluted primary antibody against Lamin B1 (1:1000, ab16048, Abcam) and β -actin (1:2000, sc-47778, Santa Cruz). After three 10-minute washes with TBST, membranes were treated with a 1:5000 dilution of horseradish peroxidase-conjugated anti-mouse or anti-rabbit antibodies for 1 hour. Following additional TBST washes, the blots were developed using the Western blotting luminol reagent (sc-2048, Santa Cruz) per the manufacturer's instructions.

Immunocytochemistry

After growing on sterile glass coverslips in 6-well plates for 24 hours, *LMNB1*^{-/-} cell line was washed with PBS and fixed for 30 mins with 1% paraformaldehyde (PFA). The cells were permeabilized with 0.5% Triton X-100 in PBS for 30 minutes and incubated for 1 hr in a blocking solution consisting of 1% BSA in PBS containing 0.1% Triton X-100. The primary antibody against ETS1 (1:100, 14069S, Cell Signaling Technology) was incubated

overnight at 4 °C and subsequently washed with 0.1% Triton X-100 in PBS. The secondary antibody was applied and incubated for 1 hour at room temperature (RT) in the dark. Nuclei were counterstained with 3 µg/ml 4',6-diamidino-2-phenylindole (DAPI) for 3 minutes at RT in the dark. Fluorescence signals were detected with a confocal microscope (Nikon Ti2-E) and analyzed with the 'NIS-elements BR program' (v.5.21.00, Nikon, Japan). Fluorescence signals of the nucleus size and intensity were measured by using 'The NIS-Elements BR program (v.5.21.00, Nikon, Japan). The fluorescent intensity of confocal images was quantified per cell by using Imaris software 10.2.0 (Oxford Instruments) cell module.

Bioinformatical analysis using GEPIA2

A total of 212 genes involved in the RNA splicing process (MSigDB: Reactome mRNA Splicing) were put into GEPIA2 (<http://gepia2.cancer-pku.cn/#index>) (Tang et al. 2017) as signatures and calculated the correlation with *ETS1* and *LMNB1*.

Gene ontology and GSEA analysis

DAVID (<http://david.abcc.ncifcrf.gov>) (Huang da et al. 2009) allowed significant DEGs and the target genes of *ELF1*, *ETS1*, *ELK3*, and *ELK4* in respective gene sets to be clustered into functional gene ontologies. Enriched gene ontology terms were identified using Metascape, and scatter plots of ontology terms were made using REVIGO (Supek et al. 2011). GSEA analysis was performed using (GSEA 4.3.3; <http://www.broadinstitute.org/gsea/index.jsp>) with MsigDB v2024.1.Hs human database and v2024.1.Mm mouse database.

Statistical analysis

GraphPad PRISM statistical software was utilized to assess the significance of differences between the results using Student's t-test. The data are presented as mean ± standard error of the mean (SEM) and were derived from two or three independent experiments. *P* values less than 0.05 were considered statically significant.

Extraction target genes and promoter sequences

The target genes of *ELF1*, *ETS1*, *ELK3*, and *ELK4* were extracted from CHEA database (<https://maayanlab-cloud/Harmonizome/dataset/CHEA+Transcription+Factor+Targets>) (Lachmann et al. 2010). The promoter sequences of splicing factor genes with FPKM > 5 in

MRC5 cells (177 genes) were extracted from EPD (<https://epd.expasy.org/epd/>) (Perier et al. 1999).

Motif discovery

The promoter sequences of splicing factor genes were analyzed using the *de novo* motif finder MEME-ChIP (<http://meme.nbcr.net/meme/tools/meme-chip>, date last accessed, July 2015) (Ma et al. 2014). Also, the motif binding probabilities on promoter regions were obtained via MEME-Suite.

Hi-C-seq data visualization

We used Iterative Correction and Eigenvector decomposition (ICE) normalized Hi-C contact matrices provided by Chang, Lei *et al* (GSE124409) (Chang et al. 2022) to analyze the contact frequency in WT and *LMNB1*^{-/-} MDA-MB-231 cells. ICE-normalized matrices at a 40 Kb resolution were visualized as heatmaps to represent the contact frequencies.

To assess interaction changes, we calculated the log₂ fold change (FC) for each bin pair, comparing WT and *LMNB1*^{-/-} cells. The interaction changes were further smoothed by averaging the log₂FC values across a 5 × 5 grid (25 bins) centered on each bin, followed by plotting the results on heatmaps for visualization. For TAD analysis, insulation scores were calculated for each 40 Kb bin, and TAD boundaries were determined at the valleys of the insulation profiles. Boundaries with an FDR exceeding 1 × 10⁻⁶ and TADs smaller than 200 Kb were excluded for further analysis.

Results

Depletion of Lamin B1 induces extensive misregulation of splicing factors

To examine the impact of Lamin B1 depletion, we generated MRC5 cells lacking Lamin B1 (*LMNB1*^{-/-}) using the CRISPR-Cas9 system (Supplementary Figure S1A). The complete loss of Lamin B1 was confirmed by western blot and RT-qPCR analysis (Supplementary Figure S1B, C). RNA sequencing (RNA-seq) was then conducted to assess gene expression profiles in both WT and *LMNB1*^{-/-} cells, identifying 813 significantly differentially expressed genes (DEGs) (*P* val < 0.01, absolute log₂-fold change > 0.3) in *LMNB1*^{-/-} cells. Gene ontology (GO) analysis showed that 711 downregulated genes were linked to biological processes such as mRNA processing, transcription, apoptosis, and chromatin remodeling (Figure 1A).

To explore the global role of Lamin B1 across different cell types and species, we re-analyzed publicly available

RNA-seq data from *LMNB1*-depleted MDA-MB-231 and MLE12 cells (Jia et al. 2019; Chang et al. 2022) (Figure 1B, Supplementary Figure S1D). GO analysis of significantly downregulated genes across the three *LMNB1*-deficient cell types (MRC5, MDA-MB-231, and MLE12) identified nine common functional categories consistently downregulated in all cases: RNA splicing, mRNA transport, chromatin remodeling, positive and negative

regulation of transcription by RNA polymerase II, positive and negative regulation of apoptosis, cell cycle regulation, and protein stabilization (Figure 1C).

Defects in RNA splicing can have widespread effects on gene expression and protein levels, and recent studies have highlighted the functional connection between Lamin B1 depletion and RNA splicing events in human cells (Bartoletti-Stella et al. 2015; Camps

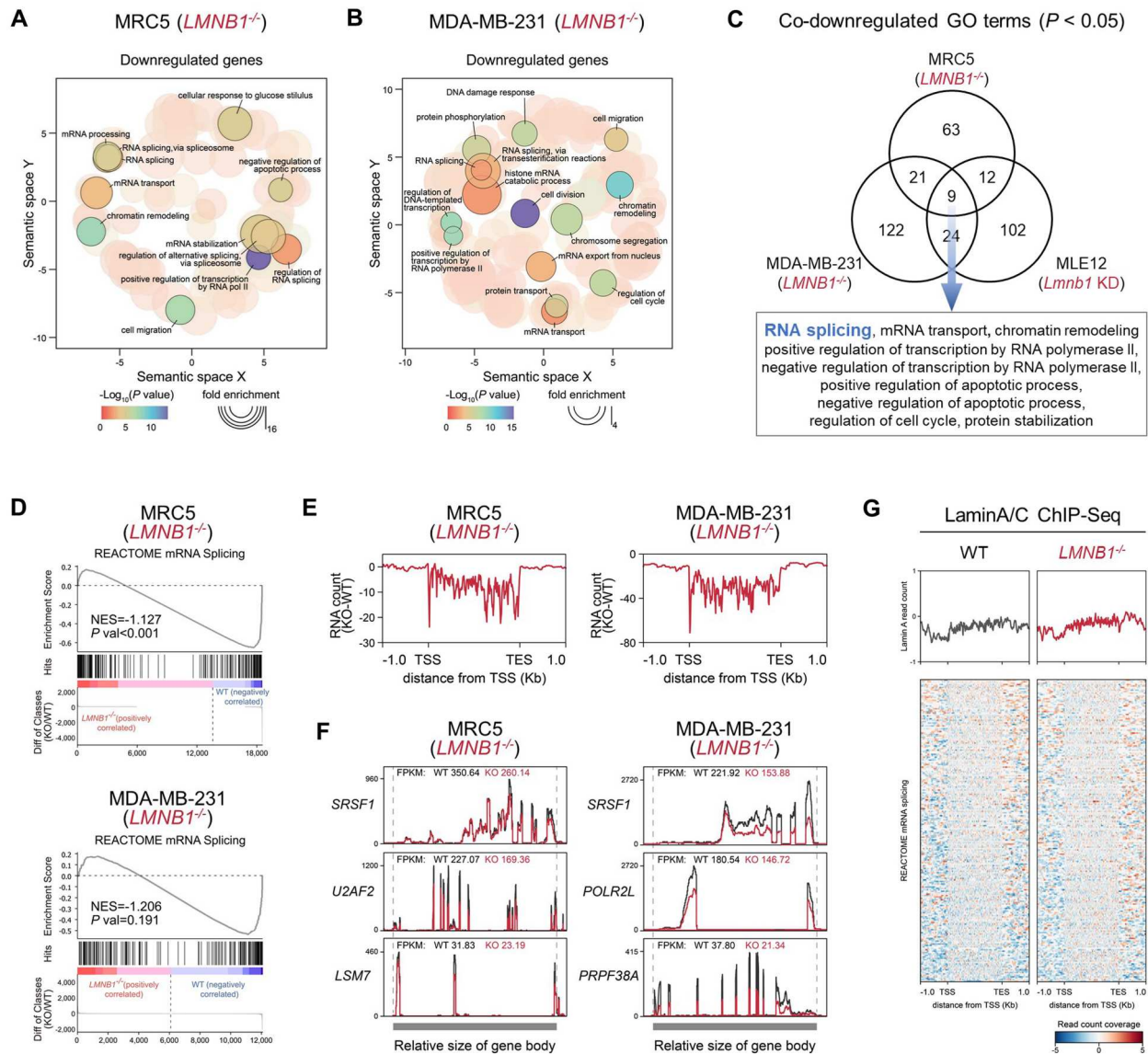


Figure 1. Loss of Lamin B1 induces global downregulation of splicing factors. (a) Statistically significant down-regulated DEGs in *LMNB1*^{-/-} MRC5 cells are obtained by following filtering criteria: $\log_2FC > 0.3$, P value < 0.01 . Gene ontologies of biological processes for down-regulated 725 DEGs are visualized. (b) Significantly down-regulated DEGs in *LMNB1*^{-/-} MDA-MB-231 cells are obtained ($\log_2FC > 0.3$, P value < 0.001). Functional clustering of 2609 DEGs are visualized. (c) GO terms are observed for the downregulated gene in *LMNB1*^{-/-} MRC5, *LMNB1*^{-/-} MDA-MB-231, and *Lmn1* KD MLE12 cells respectively, and nine terms are overlapped in three Lamin B1 depleted cells. (d) Gene set enrichment analysis (GSEA) plots for the gene set of 'Reactome mRNA splicing' in *LMNB1*^{-/-} MRC5 (top) and *LMNB1*^{-/-} MDA-MB-231 (bottom). (e) Averaged RNA count profiles for the splicing factors are compared between WT and *LMNB1*^{-/-} MRC5 (left) and MDA-MB-231 cells (right). Subtracted RNA counts (*LMNB1*^{-/-} - WT) are shown for the gene body region of splicing factors. (f) Representatives of splicing factors downregulated in *LMNB1*^{-/-} MRC5 (left) and MDA-MB-231 cells (right). RNA counts for each gene is plotted on the relative gene body region and FPKM values are indicated. (g) Profile and heatmap view of normalized Lamin A ChIP-seq signal intensity on gene body regions of splicing factors detected in WT (left) and *LMNB1*^{-/-} (right) MDA-MB-231 cells.

et al. 2015). Therefore, we focused our subsequent analysis on the role of Lamin B1 in RNA splicing in humans. Gene set enrichment analysis (GSEA), which evaluates cumulative changes in genes associated with specific biological pathways, confirmed that Lamin B1 deficiency significantly reduced the expression of genes involved in mRNA splicing, with 79.2% of such genes being downregulated in *LMNB1*^{-/-} MRC5 cells (Figure 1D, top, Supplementary Figure S1E). Similarly, in MDA-MB-231 cells, the loss of Lamin B1 led to a predominant downregulation of genes involved in RNA splicing (57.7%), while 42.3% showed a slight increase in expression (Figure 1D, bottom, Supplementary Figure S1F).

Consistently, the average RNA-seq read counts for mRNA splicing factors were lower in *LMNB1*^{-/-} cells than WT cells (Figure 1E). For example, the read counts and FPKM values for splicing factors, such as the *SRSF1* gene (Figure 1F), were significantly downregulated in *LMNB1*^{-/-} cells, indicating that the loss of Lamin B1 results in a global reduction of splicing factor expression. The downregulation of splicing factors in *LMNB1*^{-/-} cells was validated by RT-qPCR, showing remarkable consistency with RNA-seq results (Supplementary Figure S2A, B).

These findings were further corroborated by analyzing the relationship between Lamin B1 and splicing factor expression using the GEPIA database (<http://gepia2.cancer-pku.cn/#index>). We input 212 mRNA splicing-related genes into GEPIA as a signature to assess their correlation with *LMNB1* expression (Supplementary Figure S3). The results showed a significant positive correlation between the expression of splicing factors and *LMNB1* across various tissues, reinforcing the connection between Lamin B1 and the regulation of splicing factor expression.

Lamin B1 is believed to create a repressive environment for transcription regulation at the nuclear lamina, and changes in the proximity between chromatin and the lamina can influence the expression of specific genes (Peric-Hupkes et al. 2010; Robson et al. 2016; Lim et al. 2024). To investigate whether the loss of Lamin B1 altered the spatial positioning of splicing factor gene loci near the nuclear lamina, we compared Lamin A ChIP-Seq signals between WT and *LMNB1*^{-/-} MDA-MB-231 cells (Figure 1G). However, the spatial positioning of splicing factor genes did not show reduced interactions with the nuclear lamina, suggesting that an unknown mechanism underlies the selective downregulation of splicing factors in *LMNB1*^{-/-} cells.

Promoters of splicing factors are firmly bound by the ETS transcription factor family

Since Lamin B1 depletion selectively reduced the expression of splicing factors without affecting their

association with the nuclear lamina, we hypothesized that the loss of Lamin B1 might alter the expression of an upstream transcription factor (TF) that regulates splicing factors. Through de novo motif analysis using MEME-ChIP, we identified an enriched DNA sequence in the promoter regions of splicing factors (Figure 2A, B; Supplementary Figure S3). This sequence closely matched the binding motifs of ZBTB7A, ZNF93, and 17 proteins from the ETS transcription factor family, the primary group with the most significant *E*-value (Figure 2B). Secondary ranked groups included binding motifs for YY1, YY2, and ZFP42, also in the promoter regions of splicing factors (Supplementary Figure S4B). However, YY2 and ZFP42 were not expressed in WT MRC5 cells (FPKM = 0) (Supplementary Figure S4C). In the case of YY1, its expression was not significantly decreased in *LMNB1*^{-/-} MRC5 cells, which was further validated by RT-qPCR (Supplementary Figure S4D), suggesting that the factors in the secondary group do not have a regulatory role in normal cells.

Next, we established two criteria to identify potential regulators of splicing factors: (1) expression levels above a specified threshold in WT cells (FPKM > 10) and (2) reduced expression in *LMNB1*^{-/-} cells (\log_2 -fold change < -0.3). Among the 19 transcription factors (TFs) identified by MEME-ChIP, only four (ELF1, ELK3, ELK4, and ETS1) met both criteria in *LMNB1*^{-/-} MRC5 and MDA-MB-231 cells (Figure 2C, Supplementary Figure S4E). The binding motifs for these four TFs corresponded to the DNA sequences identified in the MEME analysis (Figure 2D), and their predicted binding occupancy was enriched in the promoter regions of splicing factors (Figure 2E). Finally, we identified potential target genes for each TF among the splicing factors (Figure 2F). The splicing factors that are potentially regulated by ELF1, ELK3, ELK4, or ETS1 were consistently downregulated in *LMNB1*^{-/-} cells, suggesting that one or more of these TFs may function as regulators of splicing factors.

ETS1 target genes are highly involved in splicing processes

To compare the potential regulatory roles of the four transcription factors (TFs) on splicing factor genes, we next analyzed the functional clusters of the target genes for each TF. Utilizing the CHEA transcription factor targets database (Lachmann et al. 2010; Keenan et al. 2019), we identified target genes for each TF (ELF1: 1119 genes; ETS1: 1586 genes; ELK3: 1683 genes; and ELK4: 350 genes). Notably, GO analysis indicated that only the target genes of ETS1 were significantly associated with RNA processing (Figure 3A-D). Among the most enriched

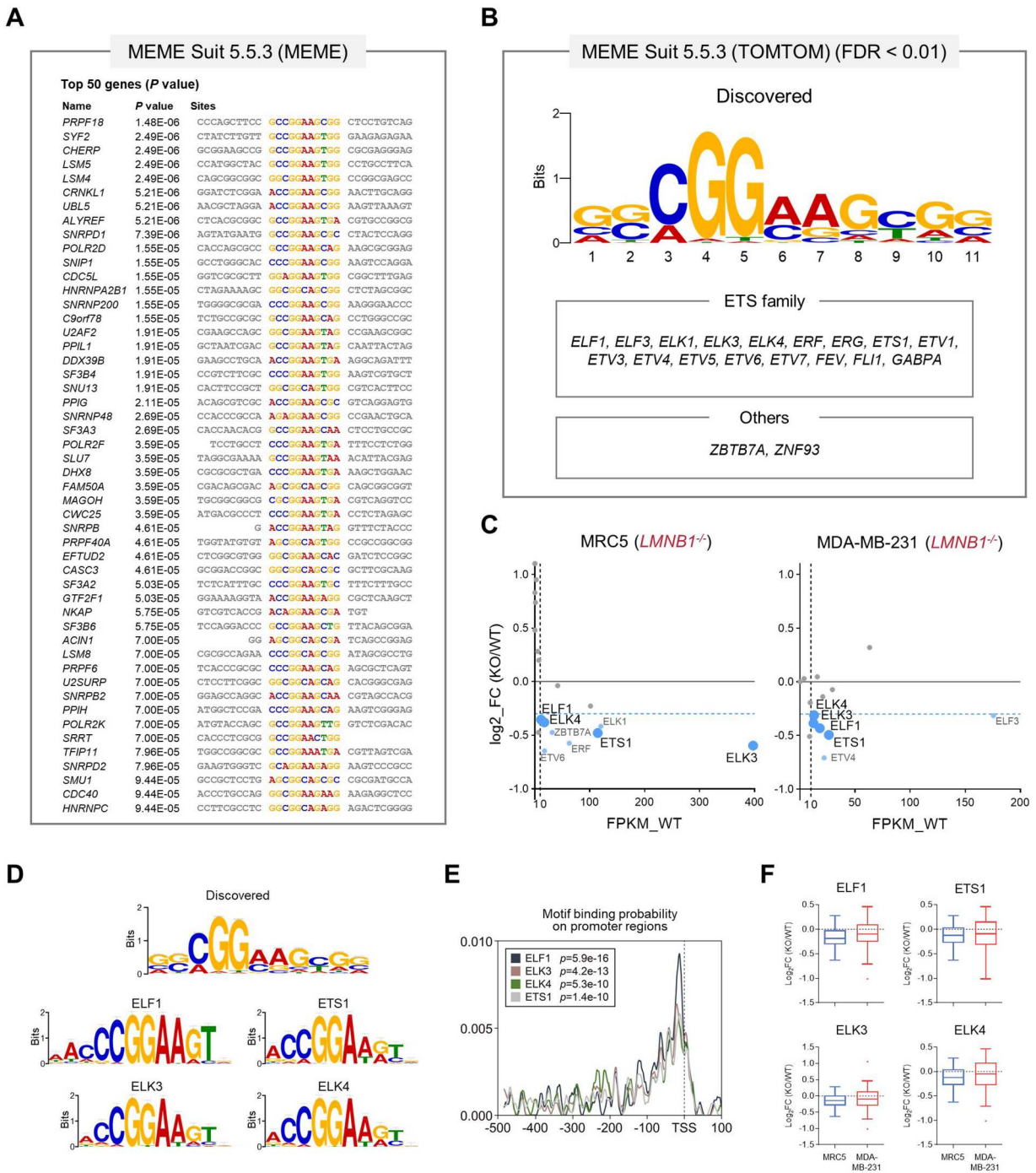


Figure 2. *De novo* discovery of putative master regulator for splicing factors. (a) MEME ChIP identifies overlapped DNA motif sequences for the promoter region of 177 slicing factors and the sequence of top 50 genes are indicated. (b) TOMTOM discovers common motif based on 'JASPAR2022 CORE vertebrates' database. Binding motifs of nineteen TFs are identified. (c) The expression of nineteen discovered TFs in WT cells and their expression changes in *LMNB1*^{-/-} MRC5 (left) and MDA-MB-231 cells (right) are shown. Genes showing FPKM > 10 in WT and reduced expression *LMNB1*^{-/-} cells ($\log_2FC < -0.3$) are shown in blue dots and 4 genes (*ELF1*, *ETS1*, *ELK3*, and *ELK4*) satisfying criteria in both MRC5 and MDA-MB-231 cells are represented in large blue dots. (d) Binding motifs of *ELF1*, *ETS1*, *ELK3*, and *ELK4* are compared with DNA sequence discovered by TOMTOM. (e) Motif binding probability of each TF (*ELF1*, *ETS1*, *ELK3*, and *ELK4*) is provided by Centrimo and represented on the promoter regions of splicing factors. (f) Putative target splicing factors are predicted for *ELF1*, *ETS1*, *ELK3*, and *ELK4* based on the sequence similarity. Expression changes (\log_2FC of FPKM compared to WT) of putative target genes are represented for *LMNB1*^{-/-} MRC5 (blue) and MDA-MB-231 (red) cells, respectively. Box represents interquartile range (IQR) and whiskers were plotted with the Tukey method.

GO terms, four of the top ten clusters for ETS1 target genes were related to RNA splicing or processing (Figure 3A-D, right). The significant downregulation of ETS1 expression in *LMNB1*^{-/-} cells was confirmed through immunocytochemistry (Supplementary Figure S5A).

Furthermore, the expression of *LMNB1* is positively correlated with that of *ETS1* across various human tissues. (Supplementary Figure S5B).

To determine whether ETS1 binds to the promoter regions of splicing factors across different human cell

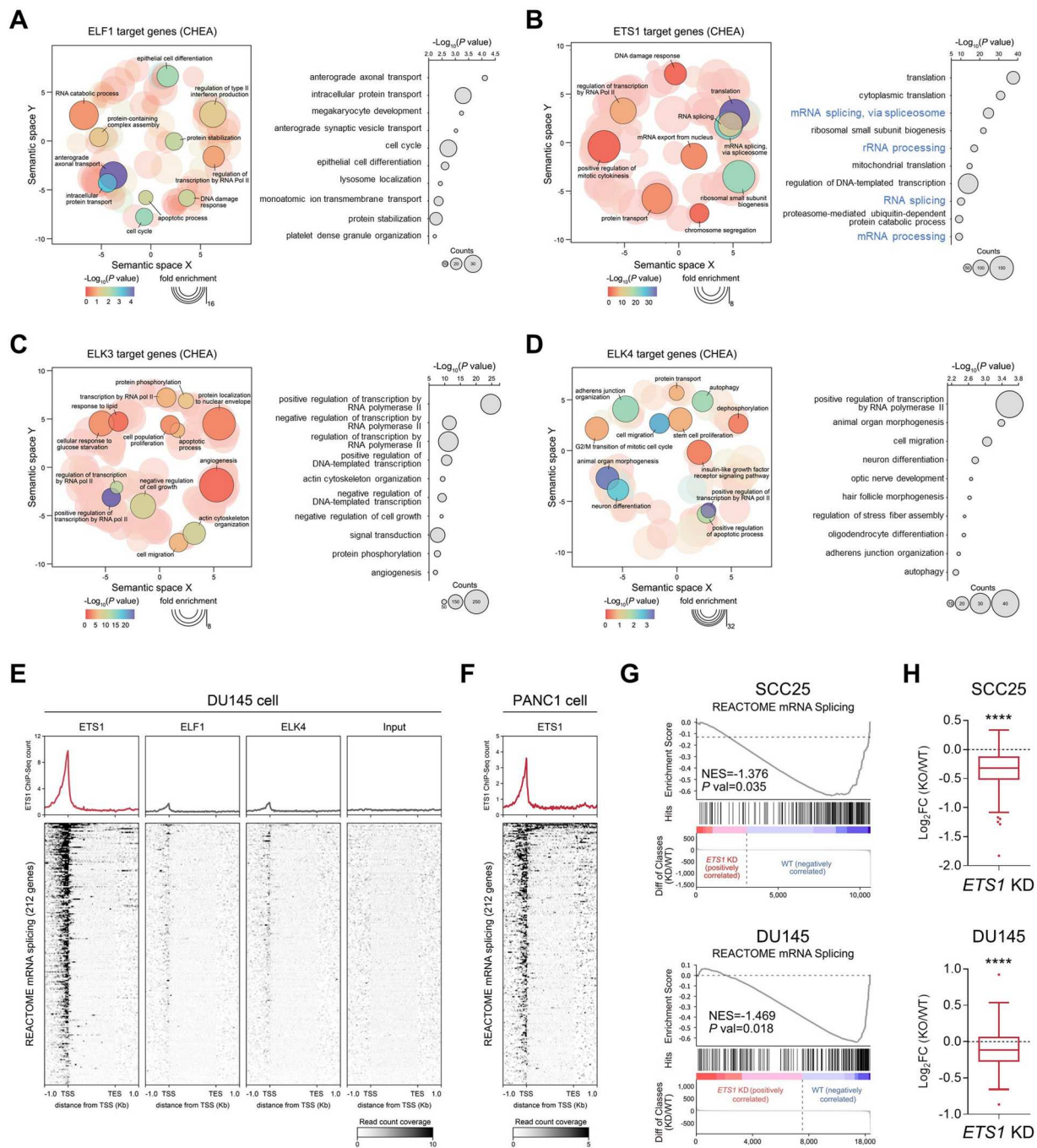


Figure 3. Among ETS family, ETS1 target genes are highly involved in splicing processes. (a-d) Target genes of ELF1 (a), ETS1 (b), ELK3 (c), and ELK4 (d) are obtained from 'CHEA Transcription Factor Targets' database and gene ontologies of biological processes for each gene set are visualized by REVIGO. (e) Profile and heatmap view of ETS1, ELF1, and ELK4 ChIP-seq and input signal intensity on ± 1 Kb of gene body regions of splicing factors in WT DU145 cells. (f) Profile and heatmap view of ETS1 ChIP-seq signal intensity on ± 1 Kb of gene body regions of splicing factors in WT PANC1 cells. (g) GSEA plots for the gene set of 'Reactome mRNA splicing' in *ETS1*^{-/-} SCC25 (top) and *ETS1*^{-/-} DU145 cells (bottom). (h) Gene expression changes (\log_2 FC of FPKM compared to WT) of actively expressed splicing factors (FPKM > 10 in WT) are shown in *ETS1*^{-/-} SCC25 (top) and *ETS1*^{-/-} DU145 cells (bottom). Error bars show mean \pm SEM. P values were calculated using two-tailed and unpaired Student's t-test. ****P < 0.0001.

types, we re-analyzed publicly available ChIP-seq data for ETS1 in two human cell lines (DU145 and PANC1). In DU145 cells, ETS1 was strongly enriched at nearly all promoter regions of splicing factors (Figure 3E). In contrast, when examining the binding capacity of ELF1 and ELK4, another potential regulator, the ChIP-seq

signals for these transcription factors, were nearly absent in the promoter regions of splicing factors in the input samples. Similarly, ETS1 was also found to occupy the promoter regions of splicing factors in PANC1 cells. The specificity of ETS1 binding to splicing factor promoters was further validated by comparing

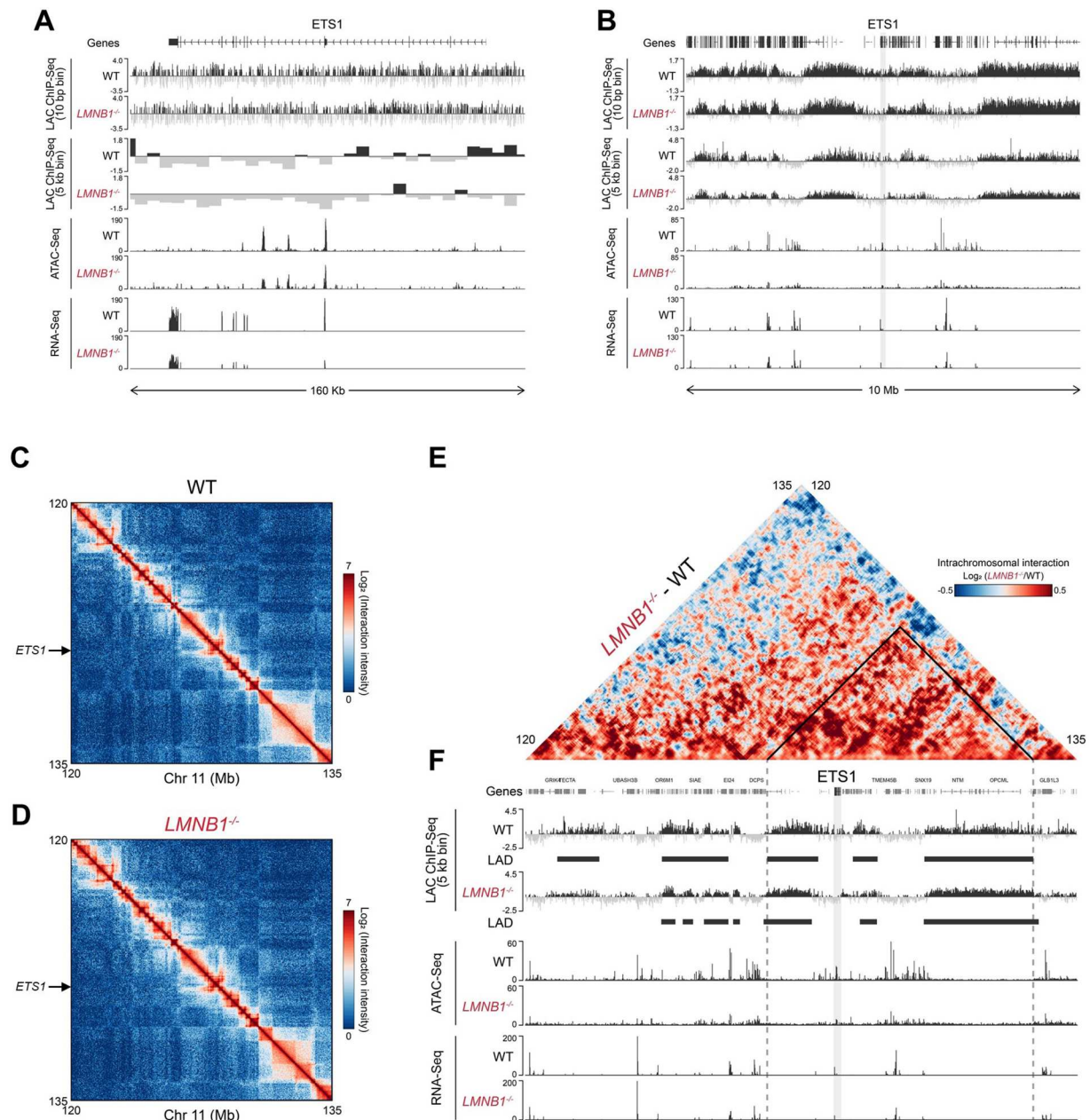


Figure 4. Lamin B1 depletion alters inter-LAD interaction adjacent to *ETS1* gene locus followed by diminished expression. (a and b) Tracks of Lamin A ChIP-seq (10 bp and 5 kb bin), ATAC-seq, and RNA-seq in WT and *LMNB1*^{-/-} MDA-MB-231 cells. Signal intensity peaks in a 160 kb (a) and 10 Mb region (b) centered around the *ETS1* gene locus are represented. (c and d) Iterative correction and eigenvector decomposition (ICE)-normalized contact frequencies are visualized in 40 kb binned heatmaps. Contact frequencies in a representative region (Chr11 120–135 Mb) are shown in WT (c) and *LMNB1*^{-/-} (d) MDA-MB-231 cells. (e) Smoothed (5 bin) heatmaps showing the log₂FC of interactions between WT and *LMNB1*^{-/-} MDA-MB-231 cells in a same representative region (Chr11 120–135 Mb). Black line indicates area with increased inter-LAD interactions in the loss of Lamin B1. (f) Tracks of Lamin A ChIP-seq (5 kb bin), Lamina associated domain (LAD), ATAC-seq, and RNA-seq in WT and *LMNB1*^{-/-} MDA-MB-231 cells. Gene locus of *ETS1* is shaded with light gray and LAD boundaries adjacent to *ETS1* are marked with dashed line.

the ChIP-seq signals of ETS1 on the promoter regions of 212 randomly selected genes (Supplementary Figure S6A, B). The binding occupancy of ETS1 on these random gene promoters was significantly lower than that on splicing factor promoters in both DU145 and PANC1 cells.

Finally, we examined the expression relationship between ETS1 and splicing factors using GEPIA and publicly available datasets. The signature scores of splicing factors exhibited a significant positive correlation with ETS1 expression, supporting the role of ETS1 in regulating these factors (Supplementary Figure S6C). Additionally, GSEA analysis following ETS1 knockdown (KD) in SCC25 and DU145 cells showed that the depletion of ETS1 resulted in a substantial misregulation of splicing factors (Figure 3G). The expression of these genes was significantly reduced after the loss of ETS1 in both human cell lines (Figure 3H), demonstrating that ETS1 functions as a regulator of a subset of genes involved in RNA splicing processes in human cells.

Lamin B1 depletion alters inter-LAD interaction adjacent to ETS1 gene locus followed by diminished expression

Given that the nuclear lamina creates a repressive environment for transcription processes, we hypothesized that the downregulation of *ETS1* was due to increased interaction between the *ETS1* gene locus and the lamina. To confirm any changes in the spatial positioning of the *ETS1* gene relative to the nuclear lamina, we compared Lamin A ChIP-seq signals between WT and *LMNB1*^{-/-} MDA-MB-231 cells. At both high- and low-resolution scales, the level of lamina association at the *ETS1* gene locus was not increased, following the loss of Lamin B1 (Figure 4A, B). Interestingly, chromatin accessibility and RNA expression of genes adjacent to the *ETS1* locus were significantly decreased in *LMNB1*^{-/-} cells (Figure 4B), suggesting that Lamin B1 depletion altered the transcriptional activity of the larger chromatin domain encompassing the *ETS1* gene locus.

Studies have shown that alterations in inter- or intra-chromosomal interactions can influence the transcriptional activity of a chromatin domain (Zheng et al. 2018). For example, when a chromatin domain increases its interaction with active genomic regions, the expression of genes within that domain can rise, whereas interactions with repressive regions can lead to decreased expression. Thus, we hypothesized that the abnormal downregulation of *ETS1* following Lamin B1 depletion occurred either due to increased interaction with a repressive domain or decreased interaction with an active domain. Upon applying the Hi-C contact

map analysis to WT and *LMNB1*^{-/-} MDA-MB-231 cells, we found that Lamin B1 depletion did not affect the checkerboard patterns of interaction heatmaps in chromatin regions surrounding the *ETS1* gene locus (Figure 4C, D), consistent with previous reports (Zheng et al. 2018; Chang et al. 2022).

However, differential interaction matrices comparing WT and *LMNB1*^{-/-} cells ($\log_2(LMNB1^{-/-}/WT)$) revealed that the loss of Lamin B1 led to a significant increase in intra-chromosomal interactions around the *ETS1* gene locus (Figure 4E). We further integrated the locations of lamina-associated domains (LADs) identified from Lamin A ChIP-seq data to distinguish transcriptionally repressive chromatin regions (Figure 4F). Notably, *ETS1* is situated between adjacent LAD regions, and the inter-LAD interaction around *ETS1* was enhanced following Lamin B1 depletion. This change in interaction appears to create a repressive environment, subsequently reducing the expression of genes located in this region (Supplementary Figure S7A, B).

Discussion

Recent studies constantly emphasize the critical role of intra- and inter-chromatin interactions in regulating gene expression by facilitating contacts between regulatory elements, such as enhancers and promoters (Galupa et al. 2022; Balasubramanian et al. 2024). Disruption of TAD-TAD interactions has been shown to cause the dysregulation of multiple genes and increase the risk of complex diseases (Zheng et al. 2018; McArthur and Capra 2021; Galupa et al. 2022). Moreover, the depletion of Lamin proteins has been linked to alterations in intra- or inter-chromatin interactions at the levels of chromosomes (Pujadas Liwag et al. 2024), compartments (Chang et al. 2022), and TADs (Zheng et al. 2018). These findings strongly highlight the correlation between changes in chromatin interactions and gene expression regulation.

The role of Lamin B1 in chromatin organization is largely facilitated by its ability to tether chromatin directly or indirectly to the nuclear periphery (Schreiner et al. 2015). Recent studies have demonstrated that the loss of B-type Lamins influences chromatin compaction and mobility, resulting in genome-wide changes in gene expression (Chang et al. 2022; Pujadas Liwag et al. 2024). Some of the genes dysregulated by Lamin B1 depletion are involved in critical cellular functions, such as cell cycle progression, cell proliferation, and cellular senescence (Shimi et al. 2011; Klymenko et al. 2018; Lv et al. 2024). Given that Lamin B1 regulates overall genome organization rather than targeting specific gene sets, its absence

can affect not only genes with distinct functions but also upstream regulatory genes.

Our data indicate that Lamin B1 depletion led to the downregulation of ETS1, a potential upstream regulator of RNA splicing factors in human cells (Figure 3). ETS1 demonstrated a strong binding affinity for the promoter regions of splicing factors, and its expression was positively correlated with the expression of these factors. Notably, splicing factor expression was globally reduced in *LMNB1*^{-/-} human cells due to the downregulation of ETS1, without any changes in their association with the lamina (Figure 1G). These findings underscore that Lamin B1 can impact various biological processes by either directly regulating the expression of functional genes or indirectly influencing upstream regulators such as ETS1.

The *ETS1* gene locus is located between two strong lamina-associated regions, and its relative escape from the nuclear lamina allows for its active expression in wild-type MDA-MB-231 cells (Figure 4E, F). This spatial organization of the *ETS1* locus is preserved in other human cell types, including H1 (hESC), HFFc6, and K562 cells (data not shown). A previous study indicated that weak lamina-associated regions are more susceptible to the absence of Lamins, resulting in altered 3D chromatin interactions and changes in the expression of neighboring genes (Zheng et al. 2018). In line with this, our findings demonstrate that Lamin B1 depletion increased chromatin interactions between the *ETS1* locus and adjacent LADs, leading to the downregulation of *ETS1*. Given that *ETS1* expression was downregulated in both *LMNB1*^{-/-} MRC5 and MDA-MB-231 cells (Figure 2C), these results suggest that *ETS1* expression is highly sensitive to Lamin B1 levels across various human cell types. However, a few genes adjacent to *ETS1* did not show significant downregulation despite the increased interaction with LAD regions (Supplementary Figure S7A, B). This variation in expression changes may be attributed to their location in distinct Topologically Associating Domains (TADs), the basic units of chromatin folding. For example, although the *SNX19* gene is located near *ETS1*, the two genes showed opposite expression changes upon Lamin B1 depletion, likely due to their separation into distinct TADs. Further studies examining chromatin properties with various epigenetic markers are needed to determine whether alterations in 3D chromatin organization in the loss of Lamin B1 contribute to the transcriptional regulation of genes near the *ETS1* locus, particularly through changes in spatial proximity to repressive LAD regions.

Lamin B1 expression decreases with age, particularly during cellular senescence (Garvalov et al. 2019).

This decline contributes to nuclear lamina disorganization and alters chromatin interactions, leading to changes in the expression of multiple genes, including ETS1. In accordance with the reduction of Lamin B1, a recent study found that ETS1 expression was also diminished in aged individuals (long-lived individuals) compared to controls (Xiao et al. 2022). Given that ETS1 is crucial for cell survival by regulating key cell-cycle drivers such as cyclin E and CDK2 (Dittmer 2003; Wei et al. 2009; Singh et al. 2011), these findings collectively suggest a relationship between the reduction of Lamin B1, subsequent downregulation of ETS1, and age-related cellular dysfunctions. Furthermore, spliceosome dysfunction and aberrant splicing events are more prevalent during aging (Bhadra et al. 2020), which may also result from decreased Lamin B1 levels.

RNA splicing is a vital process in gene expression that generates mature mRNA, and defects in splicing can lead to mRNA degradation via nonsense-mediated decay (NMD) and the production of dysfunctional proteins or abnormal protein isoforms (Maquat 2004; Baralle and Giudice 2017). The concentration balance of splicing factors is crucial for properly utilizing splicing sites, and imbalances are commonly observed in human tumors (Hanamura et al. 1998; Liu et al. 2013; Urbanski et al. 2018). In line with our findings, RNA-seq analysis of *LMNB1*^{-/-} MDA-MB-231 and *ETS1* KD SCC25 cells identified 3,228 and 2,446 genes with differentially spliced transcripts, respectively. Notably, this gene set includes *LMNA*, another major member of the Lamin subfamily, which produces Lamin A and Lamin C isoforms through alternative splicing (Dechat et al. 2008). In *LMNB1*^{-/-} MDA-MB-231 cells, the expression level of Lamin A increased ($\log_2FC = 0.27$), while Lamin C was significantly downregulated ($\log_2FC = -0.66$) (Supplementary Figure S7C). These results suggest that Lamin B1 also plays an indirect role in regulating splicing, helping to maintain the expression balance between Lamin isoforms.

In conclusion, our data highlight the role of Lamin B1 in both chromatin organization and the regulation of gene expression. Lamin B1 influences the spatial positioning and chromatin interactions of the *ETS1* gene locus, ensuring its consistent expression for properly regulating splicing factors. Given that the expression of multiple splicing factors is tightly regulated periodically during cell cycle progression (Dominguez et al. 2016), it is more efficient to co-regulate their expression through a single cue. ETS1 may play a significant role in this process; however, the interactions between ETS1 and other regulators of splicing factors require further investigation in future studies.

Acknowledgments

The study was supported by Korea Environment Industry & Technology Institute (KEITI) through 'Digital Infrastructure Building Project for Monitoring, Surveying and Evaluating the Environmental Health Program' (Grant and Award number: 2021003330007) funded by Korea Ministry of Environment (MOE). This work also supported by the National Research Foundation of Korea (NRF) grant funded by the Korea government (MIST) (Basic Research Laboratory: NRF-RS-2023-00220089; NRF-2023R1A2C1007657).

Disclosure statement

No potential conflict of interest was reported by the author(s).

Funding

This work was supported by Korea Environmental Industry and Technology Institute [grant number: 2021003330007]; National Research Foundation of Korea [grant number: NRF-RS-2023-00220089; NRF-2023R1A2C1007657].

References

- Balasubramanian D, Borges Pinto P, Grasso A, Vincent S, Tarayre H, Lajoignie D, Ghavi-Helm Y. 2024. Enhancer-promoter interactions can form independently of genomic distance and be functional across TAD boundaries. *Nucleic Acids Res.* 52:1702–1719. doi:10.1093/nar/gkad1183.
- Baralle FE, Giudice J. 2017. Alternative splicing as a regulator of development and tissue identity. *Nat Rev Mol Cell Biol.* 18:437–451. doi:10.1038/nrm.2017.27.
- Bartoletti-Stella A, Gasparini L, Giacomini C, Corrado P, Terlizzi R, Giorgio E, Magini P, Seri M, Baruzzi A, Parchi P, et al. 2015. Messenger RNA processing is altered in autosomal dominant leukodystrophy. *Hum Mol Genet.* 24:2746–2756. doi:10.1093/hmg/ddv034.
- Bhadra M, Howell P, Dutta S, Heintz C, Mair WB. 2020. Alternative splicing in aging and longevity. *Hum Genet.* 139:357–369. doi:10.1007/s00439-019-02094-6.
- Camps J, Erdos MR, Ried T. 2015. The role of lamin B1 for the maintenance of nuclear structure and function. *Nucleus.* 6:8–14. doi:10.1080/19491034.2014.1003510.
- Camps J, Wangsa D, Falke M, Brown M, Case CM, Erdos MR, Ried T. 2014. Loss of lamin B1 results in prolongation of S phase and decondensation of chromosome territories. *FASEB J.* 28:3423–3434. doi:10.1096/fj.14-250456.
- Chang L, Li M, Shao S, Li C, Ai S, Xue B, Hou Y, Zhang Y, Li R, Fan X, et al. 2022. Nuclear peripheral chromatin-lamin B1 interaction is required for global integrity of chromatin architecture and dynamics in human cells. *Protein Cell.* 13:258–280. doi:10.1007/s13238-020-00794-8.
- Dechat T, Pflieger K, Sengupta K, Shimi T, Shumaker DK, Solimando L, Goldman RD. 2008. Nuclear lamins: major factors in the structural organization and function of the nucleus and chromatin. *Genes Dev.* 22:832–853. doi:10.1101/gad.1652708.
- Dittmer J. 2003. The biology of the Ets1 proto-oncogene. *Mol Cancer.* 2:29. doi:10.1186/1476-4598-2-29.
- Dominguez D, Tsai YH, Weatheritt R, Wang Y, Blencowe BJ, Wang Z. 2016. An extensive program of periodic alternative splicing linked to cell cycle progression. *Elife.* 5:e10288. doi:10.7554/eLife.10288.
- Galupa R, Picard C, Servant N, Nora EP, Zhan Y, van Bommel JG, El Marjou F, Johanneau C, Borensztein M, Ancelin K, et al. 2022. Inversion of a topological domain leads to restricted changes in its gene expression and affects interdomain communication. *Development.* 149(9):dev200568. doi:10.1242/dev.200568.
- Garvalov BK, Muhammad S, Dobrova G. 2019. Lamin B1 in cancer and aging. *Aging (Albany NY).* 11:7336–7338. doi:10.18632/aging.102306.
- Gluck C, Glathar A, Tsompana M, Nowak N, Garrett-Sinha LA, Buck MJ, Sinha S. 2019. Molecular dissection of the oncogenic role of ETS1 in the mesenchymal subtypes of head and neck squamous cell carcinoma. *PLoS Genet.* 15:e1008250. doi:10.1371/journal.pgen.1008250.
- Goldman RD, Gruenbaum Y, Moir RD, Shumaker DK, Spann TP. 2002. Nuclear lamins: building blocks of nuclear architecture. *Genes Dev.* 16:533–547. doi:10.1101/gad.960502.
- Hanamura A, Caceres JF, Mayeda A, Franza BR, Jr., Krainer AR. 1998. Regulated tissue-specific expression of antagonistic pre-mRNA splicing factors. *RNA.* 4:430–444.
- Huang da W, Sherman BT, Lempicki RA. 2009. Systematic and integrative analysis of large gene lists using DAVID bioinformatics resources. *Nat Protoc.* 4:44–57. doi:10.1038/nprot.2008.211.
- Jia Y, Vong JS, Asafava A, Garvalov BK, Caputo L, Cordero J, Singh A, Boettger T, Gunther S, Fink L, et al. 2019. Lamin B1 loss promotes lung cancer development and metastasis by epigenetic derepression of RET. *J Exp Med.* 216:1377–1395. doi:10.1084/jem.20181394.
- Kaneshiro JM, Capitano JS, Hetzer MW. 2023. Lamin B1 overexpression alters chromatin organization and gene expression. *Nucleus.* 14(1):2202548. doi:10.1080/19491034.2023.2202548.
- Keenan AB, Torre D, Lachmann A, Leong AK, Wojciechowicz ML, Utti V, Jagodnik KM, Kropiwnicki E, Wang Z, Ma'ayan A. 2019. ChEA3: transcription factor enrichment analysis by orthogonal omics integration. *Nucleic Acids Res.* 47:W212–W224. doi:10.1093/nar/gkz446.
- Kim SJ, Park SH, Myung K, Lee KY. 2024. Lamin A/C facilitates DNA damage response by modulating ATM signaling and homologous recombination pathways. *Anim Cells Syst (Seoul).* 28:401–416. doi:10.1080/19768354.2024.2393820.
- Klymenko T, Bloehdorn J, Bahlo J, Robrecht S, Akylzhanova G, Cox K, Estenfelder S, Wang J, Edelmann J, Strefford JC, et al. 2018. Lamin B1 regulates somatic mutations and progression of B-cell malignancies. *Leukemia.* 32:364–375. doi:10.1038/leu.2017.255.
- Koedoot E, Smid M, Foekens JA, Martens JWM, Le Devedec SE, van de Water B. 2019. Co-regulated gene expression of splicing factors as drivers of cancer progression. *Sci Rep.* 9(1):5484. doi:10.1038/s41598-019-40759-4.
- Lachmann A, Xu H, Krishnan J, Berger SI, Mazloom AR, Ma'ayan A. 2010. ChEA: transcription factor regulation inferred from integrating genome-wide ChIP-X experiments. *Bioinformatics.* 26:2438–2444. doi:10.1093/bioinformatics/btq466.
- Latorre E, Ostler EL, Faragher RGA, Harries LW. 2019. Foxo1 and ETV6 genes may represent novel regulators of splicing factor expression in cellular senescence. *FASEB J.* 33:1086–1097. doi:10.1096/fj.201801154R.

- Lee GY, Ham S, Sohn J, Kwon HC, Lee SV. 2024. Meta-analysis of the transcriptome identifies aberrant RNA processing as common feature of aging in multiple species. *Mol Cells*. 47:100047. doi:10.1016/j.mocell.2024.100047.
- Li D, McIntosh CS, Mastaglia FL, Wilton SD, Aung-Htut MT. 2021. Neurodegenerative diseases: a hotbed for splicing defects and the potential therapies. *Transl Neurodegener*. 10:16. doi:10.1186/s40035-021-00240-7.
- Lim YH, Park YJ, Lee J, Kim JH. 2024. Transcriptional corepressor activity of CtBP1 is regulated by ISG15 modification. *Anim Cells Syst (Seoul)*. 28:66–74. doi:10.1080/19768354.2024.2321354.
- Liu Q, Fang L, Wu C. 2022. Alternative splicing and isoforms: from mechanisms to diseases. *Genes (Basel)*. 13(3):401. doi:10.3390/genes13030401.
- Liu Y, Conaway L, Rutherford Bethard J, Al-Ayoubi AM, Thompson Bradley A, Zheng H, Weed SA, Eblen ST. 2013. Phosphorylation of the alternative mRNA splicing factor 45 (SPF45) by Clk1 regulates its splice site utilization, cell migration and invasion. *Nucleic Acids Res*. 41:4949–4962. doi:10.1093/nar/gkt170.
- Lv T, Wang C, Zhou J, Feng X, Zhang L, Fan Z. 2024. Mechanism and role of nuclear laminin B1 in cell senescence and malignant tumors. *Cell Death Discov*. 10:269. doi:10.1038/s41420-024-02045-9.
- Ma W, Noble WS, Bailey TL. 2014. Motif-based analysis of large nucleotide data sets using MEME-ChIP. *Nat Protoc*. 9:1428–1450. doi:10.1038/nprot.2014.083.
- Maquat LE. 2004. Nonsense-mediated mRNA decay: splicing, translation and mRNP dynamics. *Nat Rev Mol Cell Biol*. 5:89–99. doi:10.1038/nrm1310.
- Maroulakou IG, Bowe DB. 2000. Expression and function of Ets transcription factors in mammalian development: a regulatory network. *Oncogene*. 19:6432–6442. doi:10.1038/sj.onc.1204039.
- McArthur E, Capra JA. 2021. Topologically associating domain boundaries that are stable across diverse cell types are evolutionarily constrained and enriched for heritability. *Am J Hum Genet*. 108:269–283. doi:10.1016/j.ajhg.2021.01.001.
- Mehlferber MM, Kuyumcu-Martinez M, Miller CL, Sheynkman GM. 2023. Transcription factors and splice factors - interconnected regulators of stem cell differentiation. *Curr Stem Cell Rep*. 9:31–41. doi:10.1007/s40778-023-00227-2.
- Oikawa T, Yamada T. 2003. Molecular biology of the Ets family of transcription factors. *Gene*. 303:11–34. doi:10.1016/S0378-1119(02)01156-3.
- Peric-Hupkes D, Meuleman W, Pagie L, Bruggeman SW, Solovei I, Brugman W, Graf S, Flicek P, Kerkhoven RM, van Lohuizen M, et al. 2010. Molecular maps of the reorganization of genome-nuclear lamina interactions during differentiation. *Mol Cell*. 38:603–613. doi:10.1016/j.molcel.2010.03.016.
- Perier RC, Junier T, Bonnard C, Bucher P. 1999. The eukaryotic promoter database (EPD): recent developments. *Nucleic Acids Res*. 27:307–309. doi:10.1093/nar/27.1.307.
- Plotnik JP, Budka JA, Ferris MW, Hollenhorst PC. 2014. Ets1 is a genome-wide effector of RAS/ERK signaling in epithelial cells. *Nucleic Acids Res*. 42:11928–11940. doi:10.1093/nar/gku929.
- Podszycalow-Bartnicka P, Neugebauer KM. 2023. Splicing under stress: A matter of time and place. *J Cell Biol*. 222(12):e202311014. doi:10.1083/jcb.202311014.
- Pujadas Liwag EM, Wei X, Acosta N, Carter LM, Yang J, Almossalha LM, Jain S, Daneshkhan A, Rao SSP, Seker-Polat F, et al. 2024. Depletion of lamins B1 and B2 promotes chromatin mobility and induces differential gene expression by a mesoscale-motion-dependent mechanism. *Genome Biol*. 25:77. doi:10.1186/s13059-024-03212-y.
- Robson MI, de Las Heras JI, Czapiewski R, Le Thanh P, Booth DG, Kelly DA, Webb S, Kerr ARW, Schirmer EC. 2016. Tissue-Specific Gene repositioning by muscle nuclear membrane proteins enhances repression of critical developmental genes during Myogenesis. *Mol Cell*. 62:834–847. doi:10.1016/j.molcel.2016.04.035.
- Saulnier O, Guedri-Idjouadiene K, Aynaud MM, Chakraborty A, Bruyr J, Pineau J, O'Grady T, Mirabeau O, Grossetete S, Galvan B, et al. 2021. Erg transcription factors have a splicing regulatory function involving RBFOX2 that is altered in the EWS-FLI1 oncogenic fusion. *Nucleic Acids Res*. 49:5038–5056. doi:10.1093/nar/gkab305.
- Schor IE, Lleres D, Risso GJ, Pawellek A, Ule J, Lamond AI, Kornblihtt AR. 2012. Perturbation of chromatin structure globally affects localization and recruitment of splicing factors. *PLoS One*. 7:e48084. doi:10.1371/journal.pone.0048084.
- Schreiner SM, Koo PK, Zhao Y, Mochrie SG, King MC. 2015. The tethering of chromatin to the nuclear envelope supports nuclear mechanics. *Nat Commun*. 6:7159. doi:10.1038/ncomms8159.
- Sementchenko VI, Watson DK. 2000. Ets target genes: past, present and future. *Oncogene*. 19:6533–6548. doi:10.1038/sj.onc.1204034.
- Sharrocks AD. 2001. The ETS-domain transcription factor family. *Nat Rev Mol Cell Biol*. 2:827–837. doi:10.1038/35099076.
- Shimi T, Butin-Israeli V, Adam SA, Hamanaka RB, Goldman AE, Lucas CA, Shumaker DK, Kosak ST, Chandel NS, Goldman RD. 2011. The role of nuclear lamin B1 in cell proliferation and senescence. *Genes Dev*. 25:2579–2593. doi:10.1101/gad.179515.111.
- Singh AK, Swarnalatha M, Kumar V. 2011. c-ETS1 facilitates G1/S-phase transition by up-regulating cyclin E and CDK2 genes and cooperates with hepatitis B virus X protein for their deregulation. *J Biol Chem*. 286:21961–21970. doi:10.1074/jbc.M111.238238.
- Supek F, Bosnjak M, Skunca N, Smuc T. 2011. Revigo summarizes and visualizes long lists of gene ontology terms. *PLoS One*. 6:e21800. doi:10.1371/journal.pone.0021800.
- Tang CW, Maya-Mendoza A, Martin C, Zeng K, Chen S, Feret D, Wilson SA, Jackson DA. 2008. The integrity of a lamin-B1-dependent nucleoskeleton is a fundamental determinant of RNA synthesis in human cells. *J Cell Sci*. 121:1014–1024. doi:10.1242/jcs.020982.
- Tang Z, Li C, Kang B, Gao G, Li C, Zhang Z. 2017. Gepia: a web server for cancer and normal gene expression profiling and interactive analyses. *Nucleic Acids Res*. 45:W98–W102. doi:10.1093/nar/gkx247.
- Urbanski LM, Leclair N, Anczukow O. 2018. Alternative-splicing defects in cancer: splicing regulators and their downstream targets, guiding the way to novel cancer therapeutics. *Wiley Interdiscip Rev RNA*. 9:e1476. doi:10.1002/wrna.1476.
- Vester K, Preussner M, Holton N, Feng S, Schultz C, Heyd F, Wahl MC. 2022. Recruitment of a splicing factor to the nuclear lamina for its inactivation. *Commun Biol*. 5:736. doi:10.1038/s42003-022-03689-y.

- Wasylyk B, Hahn SL, Giovane A. 1993. The Ets family of transcription factors. *Eur J Biochem.* 211:7–18. doi:10.1111/j.1432-1033.1993.tb19864.x.
- Wei G, Srinivasan R, Cantemir-Stone CZ, Sharma SM, Santhanam R, Weinstein M, Muthusamy N, Man AK, Oshima RG, Leone G, et al. 2009. Ets1 and Ets2 are required for endothelial cell survival during embryonic angiogenesis. *Blood.* 114:1123–1130. doi:10.1182/blood-2009-03-211391.
- Xiao FH, Yu Q, Deng ZL, Yang K, Ye Y, Ge MX, Yan D, Wang HT, Chen XQ, Yang LQ, et al. 2022. Ets1 acts as a regulator of human healthy aging via decreasing ribosomal activity. *Sci Adv.* 8:eabf2017. doi:10.1126/sciadv.abf2017.
- Yang SH, Jung HJ, Coffinier C, Fong LG, Young SG. 2011. Are B-type lamins essential in all mammalian cells? *Nucleus.* 2:562–569. doi:10.4161/nucl.2.6.18085.
- Yang Y, Han X, Sun L, Shao F, Yin Y, Zhang W. 2024. Ets transcription factors in immune cells and immune-related diseases. *Int J Mol Sci.* 25(18):10004. doi:10.3390/ijms251810004.
- Zhang J, Manley JL. 2013. Misregulation of pre-mRNA alternative splicing in cancer. *Cancer Discov.* 3:1228–1237. doi:10.1158/2159-8290.CD-13-0253.
- Zheng X, Hu J, Yue S, Kristiani L, Kim M, Sauria M, Taylor J, Kim Y, Zheng Y. 2018. Lamins organize the global three-dimensional genome from the nuclear periphery. *Mol Cell.* 71:802–815 e807. doi:10.1016/j.molcel.2018.05.017.